Reactive Blending of Functional PS and PMMA: Interfacial Behavior of in situ Formed Graft Copolymers

Z. Yin, C. Koulic, C. Pagnoulle, and R. Jérôme*

Center for Education and Research on Macromolecules (CERM), University of Liège, B6a, Sart-Tilman, B-4000, Belgium

Received October 17, 2000; Revised Manuscript Received May 7, 2001

ABSTRACT: ω-Isocyanate PMMA, α-anhydride PMMA, and PS-*co*-PSNH_2 have been prepared by atom transfer radical polymerization (ATRP) with controlled molecular weights (10^4 and 3.5×10^4) and low polydispersity (1.2). They have been used as precursors of PS-*g*-PMMA copolymers and let to react in the melt (170 °C, for 10 min) under moderate shear rate. The well-controlled molecular characteristics of these precursors are a substantial advantage to study the effect of the kinetics of the interfacial reaction on the phase morphology. When the grafting reaction is fast (NH_2/anhydride pair) and low molecular weight chains are used, the interfacial reaction is quasi-complete and a nanophase morphology is observed, whereas limited reaction and formation of microphases are observed in all the other cases. A high reaction yield requires not only that the functional groups are highly mutually reactive but also that the interface is anytime made available to the functional polymers for the reaction to progress. Then, a nanophase morphology may be observed, which is that of the copolymer formed by the interfacial reaction. A low reaction yield is dictated by either a slow interfacial reaction or a slow diffusion of the copolymer away from the interface. In the latter case, the phases formed by the unreacted precursors are stabilized by the copolymer which resides at the interface.

Introduction

Reactive blending of immiscible polymers is a useful strategy to produce organic materials with high performances. Each polymeric constituent (or part of it) must bear at least one reactive group per chain, such that a coupling reaction occurs at the interface with formation of block or graft copolymer during mixing.[1] This copolymer has a dual role when the major part of the chains are nonreactive,[2−6] i.e., reduction of the interfacial tension which is favorable to the phase breakup and stabilization of the interface which prevents the phases from coalescing. Nevertheless, the copolymer must reside at the interface for acting as an emulsifier.[7] In this respect, one benefit of the so-called reactive compatibilization is the actual formation of the compatibilizer at the interface which is the locus of collision of the mutually reactive groups.[1] In contrast, premade block or graft copolymers are initially dispersed in one phase of the blend, and they migrate to the interface only if thermodynamics and kinetics allow it.[1] This requirement also explains that in some examples of reactive compatibilization the in situ formed compatibilizer escapes from the interface where it is formed.[8] For instance, the reactive blending of end-reactive PS and PMMA (PS−COOH, $M_w = 30\,000$; PMMA−epoxy, $M_w = 20\,000$) led to large PMMA phases surrounded by clouds of micelles, whereas these micelles were no longer observed in the case of higher molecular weight precursors. The micelles can only be formed if the block copolymer leaves the interface, which clearly depends on the molecular weight of the constitutive components.[9,10] More recently, Inoue et al.[11−14] and Dedecker and Groeninckx[15] proposed that the in situ formed copolymer can be pulled out from the interfacial region, depending on the kinetics of the interfacial reaction, which controls the density of the copolymer formed at the interface at constant mixing time.[13] Whenever too many copolymer chains accumulate at the interface, they are forced to elongate perpendicularly to the interface,[16] and this entropic penalty can favor the pull-out of the copolymer chains by the shear forces.[13]

It clearly appears that reactive blending can be worked out to reach two completely different goals. If compatibilization of immiscible polymer blends is the purpose, the copolymer must reside at the interface where it is formed. Would the production of block or graft copolymer be envisioned, then the copolymer has to escape from the interface as rapidly as it is formed. The aim of this study is to focus on the effect of the coupling reaction rate on the interfacial behavior of the in situ formed graft copolymer. For this purpose, a series of end-functional PMMA, i.e., ω-isocyanate PMMA (PMMA-NCO) and α-phthalic anhydride PMMA (PMMA-anh), were prepared to react at different rates with the primary amino groups of random copolymers of styrene and α-methylstyrene substituted in the meta position by a protected primary amine (PS-*co*-PSNH_2 after deprotection). The reactive polymers were prepared by atom transfer radical polymerization (ATRP)[17] with a predicted molecular weight of 10 000 and 35 000, respectively, and a narrow molecular weight distribution. PS-*co*-PSNH_2 copolymers with two different amine contents (1.2 and 4.2 amino groups per chain) were synthesized (Table 1). At high temperature, a primary amine is expected to react irreversibly with an anhydride with formation of an imide and water. An urea is formed as result of the amine/isocyanate reaction. The reactive polymers were blended at the constant composition of 75 wt % PS and 25 wt % PMMA (Table 2).

For the sake of comparison, a set of blends was prepared with nonfunctional PS and PMMA chains. Otherwise, PS-*co*-PSNH_2 and PMMA end-capped by an isocyanate and an anhydride, respectively, were melt reacted at 170 °C for 10 min. In each blend, the molecular weight of the reactive precursors was the same, i.e., 10 000 and 35 000, respectively.

10.1021/ma001798+ CCC: $20.00
Published on Web 06/22/2001

Table 1. Polymers Used in This Study

	polymer	$M_n \times 10^{-3}$	M_w/M_n	RGC[a] (wt %)	N^r groups/ chain
A	PMMA−NCO	10	1.15		0.8
A1	PMMA−anh	10	1.2		0.9
A2	PMMA−NCO	35	1.2		0.85
A3	PMMA−anh	35	1.2		0.8
B1	PS-*co*-$PSNH_2$	10	1.1	3.3	1.2
B3	PS-*co*-$PSNH_2$	35	1.3	3.3	4.2
C1	PS	10	1.1		
C2	PS	35	1.2		
C3	PMMA	10	1.1		
C4	PMMA	35	1.2		

[a] RGC = reactive group content.

Table 2. Composition of the Blends

25 wt%	75 wt %	$M_n \times 10^{-3}$	$[NH_2]/[NCO]$ or [anh]	type of blending
PMMA−NCO	PS-*co*-$PSNH_2$	10	4.5	reactive
PMMA	PS	10		nonreactive
PMMA−anh	PS-*co*-$PSNH_2$	10	4.0	reactive
PMMA−NCO	PS-*co*-$PSNH_2$	35	14.8	reactive
PMMA	PS	35		nonreactive
PMMA−anh	PS-*co*-$PSNH_2$	35	15.8	reactive

Scheme 1. Synthesis of TMITBC

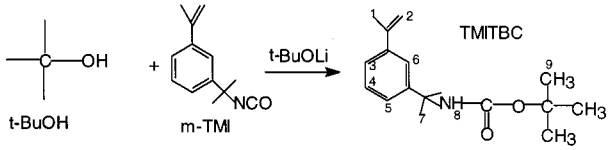

Experimental Section

Materials. 3-Isopropenyl-α,α-dimethylbenzyl isocyanate (m-TMI, see Scheme 1), and thus the comonomer precursor of the amine group in PS, was supplied by Aldrich. The radical inhibitor was removed by elution through an alumina column, and the comonomer was stored at −20 °C after bubbling of N_2. Styrene (Sty), methyl methacrylate (MMA), toluene, and *tert*-butyl alcohol (*t*-BuOH) were dried over CaH_2, distilled under reduced pressure, and stored under nitrogen at −20 °C. CuBr was purified as reported in the scientific literature.[18] It was stored under N_2 and weighed in the open air prior to polymerization. The as-received 1-phenylethyl bromide (1-PEBr, from Aldrich) (0.22 M), ethyl 2-bromoisobutyrate (EiBr, from Aldrich), 1,1,4,7,10,10-hexamethyldiethylenetriamine (HMTETA, from Aldrich) (0.37 M), and 2-hydroxyethyl 2′-methyl 2′-bromopropionate (HMB, synthesized according to Haddelton,[19] 0.33 M) were dissolved in anhydrous toluene, and the solutions were degassed by bubbling of N_2 and stored under N_2 at −20 °C. Trimellitic anhydride chloride (TAC) was stored under N_2 and used without any further purification.

Comonomer Containing a Masked Primary Amine (TMITBC). {1-Methyl-1[3-(1-methylethylenyl)phenyl]ethyl}-carbamic acid 1,1-dimethylethyl ester (TMITBC) was synthesized as shown in Scheme 1. A typical example is as follows: 5 mL of 1.0 M solution of *t*-BuOLi in cyclohexane (0.005 mol) was added dropwise to a solution of *t*-BuOH (5 mL, 0.0675 mol), 3-isopropenyl-α,α-dimethylbenzyl isocyanate (m-TMI, 11 mL, 0.05 mol), and cyclohexane (60 mL). The reaction temperature was increased to 50 °C, and the reaction progress was monitored by the decrease of the FTIR absorption of NCO at 2257 cm^{-1}. When the reaction was complete, the excess of alcohol and solvent was distilled off under reduced pressure, and a yellow-brown compound was obtained. This crude product was dissolved in 125 mL of diethyl ether, and the Li salt was quantitatively extracted by water. The monomer was isolated as a white crystal (yield 90%, mp 57 °C) upon removal of solvent. This product was characterized by ^1H NMR ($CDCl_3$ 293 K): δ 1.4 (9), δ 1.6 (7), δ 2.1 (1), δ 4.9 (8), δ 5.3 (2), δ 7.2−7.5 (3−6) ppm. Figures in parentheses refer to the protons numbered in Scheme 1.

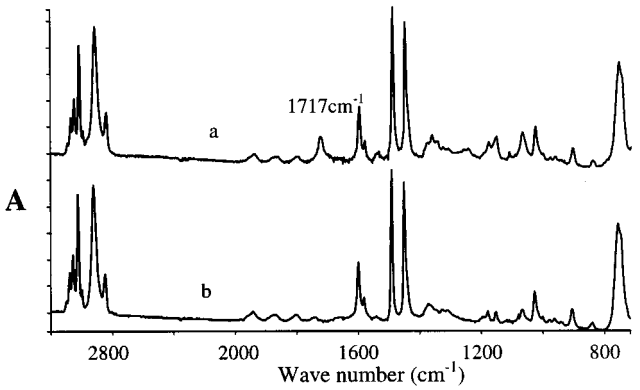

Figure 1. FTIR spectrum of poly(styrene-*co*-TMITBC) (a) and PS-*co*-$PSNH_2$ (b).

Scheme 2. Synthesis of 2-Hydroxyl-2′-ethyl-2′-bromopropionate (HMB)

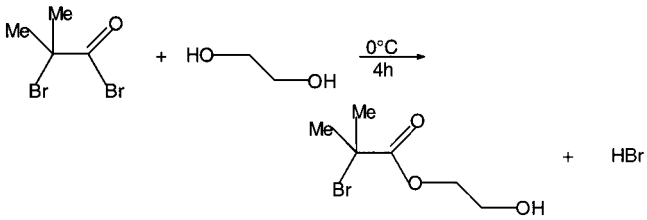

Synthesis of 2-Hydroxyethyl 2′-Methyl-2′-bromopropionate (HMB). This ATRP initiator was synthesized according to Scheme 2. Bromoisobutyryl bromide was reacted with cold anhydrous ethylene glycol (excess) under stirring for 4 h. The molar ratio of ethylene glycol and bromobutyryl bromide was 25 in order to avoid coupling reaction. The reaction mixture was added to deionized water, and the reaction product was extracted by dichloromethane. The organic solution was washed with water and sodium carbonate and dried over anhydrous magnesium sulfate. The final product was isolated as a colorless liquid upon removal of the solvent, and it was vacuum-distilled at 64.5 °C and 0.1 Torr. It was characterized by ^1H NMR ($CDCl_3$, 293 K): δ 4.3 (t, 2H), δ 3.85 (t, 2H), δ 3.0 (s, 1H); δ 1.94 (s, 6H).

Polymer Synthesis and Characterization. The molecular characteristics of the polymers used in this study are listed in Table 1. Molecular weight and molecular weight distribution were analyzed by size exclusion chromatography (SEC) in THF at 40 °C, using a Hewlett-Packard 1090 liquid chromatograph equipped with a dual Hewlett-Packard 1037A refractive index and UV detector. PMMA and PS standards (from Polymer Laboratory) were used for calibration. Before SEC analysis, the polymers were purified by elution through an alumina column.

PS-*co*-$PSNH_2$ was prepared by atom transfer radical polymerization (ATRP) of a mixture of styrene and TMITBC (3.3 wt %) at 110 °C. 1-Phenylethyl bromide was the initiator and CuBr/ HEMTETA the catalyst. The presence of carbamate groups (1717 cm^{-1}) in the PS chains was confirmed by FTIR in Figure 1a. The carbamate groups of the poly(styrene-*co*-TMITBC) were derivatized into primary amines by deprotection in a (2/1 v/v) dioxane−HCl (12 M) mixture at room temperature. The medium was then neutralized with ammonia and NaOH. The FTIR absorption of the carbamate (1717 cm^{-1}) disappeared completely as shown in Figure 1b. The amine content was thus predetermined by the carbamate content (wt %) of the poly(styrene-*co*-TMITBC) copolymer, which was measured by FTIR (Perkin-Elmer 1720X spectrometer operating in the transmission mode) on the basis of a calibration curve. For this purpose, blends of PS and TMITBC of various molar composition were dissolved in chloroform and solvent cast on a NaCl disk. The absorption of the aromatic C=C (1600 cm^{-1}) over the carbamate absorption (1717 cm^{-1}), i.e., A_{aro}/A_{carb}, was plotted vs the styrene/TMITBC molar ratio ($A_{aro}/A_{carb} = 0.147 + 0.036$[sty/TMITBC]).

Scheme 3. Synthesis of PMMA-anh

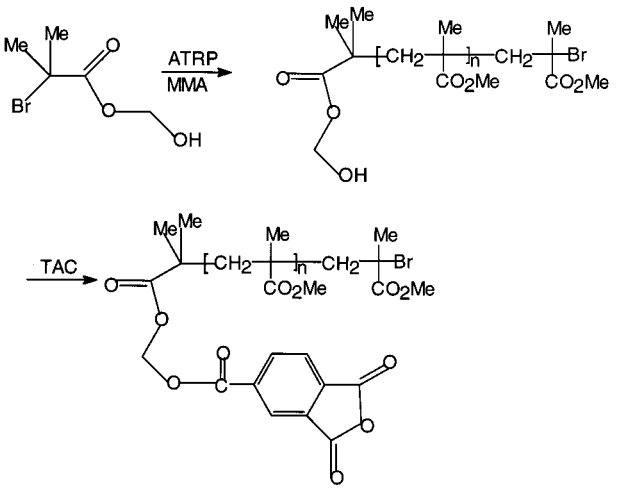

End-Capping of PMMA by an Anhydride (PMMA-anh): Hydroxyl-terminated PMMA was first prepared by ATRP of MMA at 85 °C by using HMB as an initiator and CuBr/HMTETA as a catalyst (Scheme 3). This hydroxyl end group was then reacted with trimellitic anhydride chloride (TAC) in order to end-cap PMMA by an anhydride. The inset in Figure 2 shows the resonance of the aromatic ring of the anhydride end group (7.7−8.6 ppm). The functionality of PMMA-anh was calculated from the ^{1}H NMR spectrum (Figure 2); 0.94 end group per chain was found.

End-Capping of PMMA by an Isocyanate. The ATRP of MMA was initiated by ethyl 2-bromoisobutyrate in the presence of CuBr/HMTETA in toluene at 85 °C. When the conversion was ca. 85%, excess of m-TMI (3-isopropenyl-α,α-dimethylbenzyl isocyanate) was added into the polymerization medium. Because m-TMI cannot polymerize under these conditions, it is an end-capping agent.[20] The isocyanate end group of PMMA was confirmed by the FTIR absorption of 2258 cm^{-1}. The isocyanate group was further reacted with 9-methyl-(aminomethyl)anthracene in order to measure the NCO functionality by UV.[21] An average of one end group per chain was found.

Melt Mixing. Blends were prepared in the melt with an ARES rheometer (strain controlled) between parallel plates of 25 mm diameter under a steady shear rate of 6.28 s^{-1}. Ca. 0.7 g of finely precipitated and dried precursors was dry blended before being shaped as a disk (at room temperature under 20 MPa pressure). The disk was placed between the parallel plates of the rheometer prior to apply a normal force of 20 g and to increase the temperature up to 170 °C. When the temperature was stabilized (3 min), a steady shear rate (6.28 rad s^{-1}) was applied for a fixed time. After mixing, the sample was cooled at zero shear rate and constant strain.

Conversion of the Interfacial Reaction. The reaction progress was monitored by SEC according to a method reported by Macosko et al.[22] For this purpose, phenyl isocyanate was added to the samples for quenching the unreacted amino groups and preventing these groups from being adsorbed on the SEC columns.

Phase Morphology. The phase morphology was observed with a Philips CM 100 transmission electron microscope (TEM). A Reichert-Jung Ultracut FC4 microtome equipped with a diamond knife was used to prepare ultrathin samples (ca. 50 nm), cut at the same distance, ca. 3/4 of the radius from the center of the disk (20 mm), and stained by exposure to RuO_4 vapor for 30 min. PS was observed as the darker phase, as result of the high affinity of PS for RuO_4. The size and size distribution of the dispersed phases were quantitatively analyzed with a computerized image analyzer (KS 100 Kontron imaging system). A total of 300−500 dispersed domains were considered per sample. The cross-sectional surface area of these particles was converted to an equivalent diameter by eq 1:

$$D_{\text{equivalent}} = (4/\pi(\text{area}))^{0.5} \quad (1)$$

TEM micrographs were 2D slices through a 3D morphology, such that D was underestimated. Because some smaller particles might be unobserved, the error was estimated at 10% or less.[23] $D_v = \sum D_i^3/\sum D_i^2$ emphasized the contribution of the larger particles.

Results and Discussion

The way the phase morphology is developed in reactive blending must depend on the kinetics of the interfacial reaction which controls the amount of the copolymer formed at the interface for a specific blending time. Moreover, the structure of the copolymer, and thus

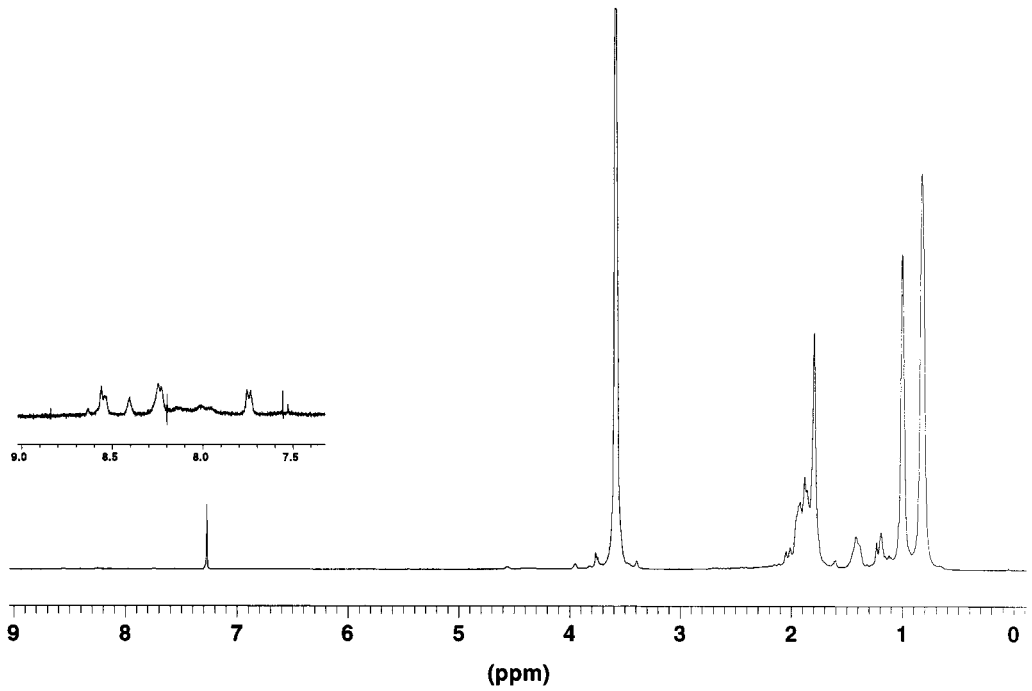

Figure 2. ^{1}H NMR spectrum of PMMA-anh (M_n = 12 000).

its interfacial activity and residence time at the interface, may not be ignored and must depend on the molecular weight of the reactive precursors and the average number of the reactive groups they contain. The influence of these two parameters—kinetics and copolymer structure—on the phase morphology is the major question addressed in this study, in which all the chains are reactive.

Blends of Reactive Precursors of Low Molecular Weight (10 000). When reactive polymers of low molecular weight (M_n = 10 000) are melt reacted, the PMMA−NCO/PS-*co*-$PSNH_2$ blend shows a slightly finer phase dispersion compared to the nonreactive counterpart after 10 min of mixing at 170 °C (Figure 3a,b). Actually, the volume average diameter (D_v) of the dispersed phases in the reactive blend ($D_{v(r)}$) is 2 times smaller compared to the nonreactive system ($D_{v(nr)}$) as reported in Table 3. Nevertheless, there is a substantial difference in the phase morphology, because the dispersed PMMA phases (white phases) contain occlusions of PS (stained by RuO_4) in the case of the reactive mixing (Figure 3b), which is never observed for the nonreactive blends. Thus, graft copolymer must be at the origin of the occlusions, either as micelles possibly swollen by unreacted PS (small size occlusions) or trapped in unreacted PS occluded in the PMMA phases (large size occlusions).

It must be noted that occlusions of the matrix in the dispersed phases were previously observed in reactive blending in the specific case of a slow interfacial reaction.[24] The poor stabilization of the phases by a too low amount of copolymer could not prevent phase coalescence from occurring and occlusions in the dispersed phases from being formed on this occasion. Figure 3b would thus be an indirect evidence for a slow NCO/NH_2 reaction. In this respect, PMMA is end-capped by a m-TMI unit (see Scheme 1), i.e., an aliphatic isocyanate which is less electrophilic than an aromatic one. Moreover, this isocyanate is sterically hindered by two methyl groups in the alpha position, which contributes to decrease further the reactivity.

To work out an intrinsically more reactive system, α-anhydride PMMA has been substituted for α-isocyanate PMMA, while keeping constant molecular weight, time, and temperature of mixing. The phase morphology of the blend is dramatically modified. Indeed, the dispersed phases are now nanometric (ca. 20 nm, Figure 3c) and no longer micrometric as was the case for the NCO/NH_2 pair (Figure 3b). This drastic modification in the phase morphology is assessed by a $D_{v(r)}/D_{v(nr)}$ ratio of 0.01 instead of 0.54 in the previous case (Table 3). This situation is reminiscent of an emulsion of PMMA in PS and, possibly, of the poorly ordered mesophases formed by a graft copolymer.[25] For the second hypothesis to be acceptable, a large enough amount of copolymer should be formed in close relation to a fast interfacial reaction. To clear up this issue, the conversion of the anhydride groups, which are used in smaller molar amount than the amines (4 times less; Table 2), has been extracted from the size exclusion chromatograms after 10 min of reaction. Table 3 shows a very high conversion of the anhydride (92%) compared to only 16.5% in the case of the isocyanate counterpart. The interfacial reaction is thus now comparatively much faster, and the blend consists of 46 wt % of copolymer, 2 wt % PMMA, and 52% PS, which is very close to the composition in the case of complete reaction (50 wt % copolymer; 50 wt % PS). According to Table 1, the reactive chains of 10 000 molecular weight contain one reactive group per chain in average. Therefore, the in situ formed copolymer must be an Y-shaped graft copolymer of M_n = 20 000 containing 50 wt % of each constituent. Figure 3c is thus representative of the phase morphology of a mixture of a graft copolymer [PS-(10 000)-*g*-PMMA(10 000)] and the same weight of one constitutive chain (PS) of the same molecular weight (10 000). Whether homo-PS completely accommodated in the PS mesophase of the graft copolymer is an open question, however, and not essential to the problem discussed in this paper. Similar morphology was reported by Orr et al.[25] for blends of 70 wt % of aliphatic amine end-capped PS and 30 wt % of anhydride end-functional polybutadiene mixed at 180 °C.

From the comparison of the PMMA−NCO/PS-*co*-$PSNH_2$ and the PMMA-anh/PS-*co*-$PSNH_2$ blends of low molecular weight (10 000), it appears that the interfacial reaction is the rate-determining step for the formation of the graft copolymer and the development of the phase morphology, rather than the diffusion of the reactive chains to the interface. Moreover, for the interfacial reaction to be complete, the interfacial area must be anytime available to the not yet reacted chains. In the case of PMMA-anh (10 000), the copolymer is rapidly formed and saturates the original interface. Two situations are then possible: either the interface is destabilized (decrease of the interfacial tension) and its area increases under the very moderate shear operating in these experiments, or the copolymer leaves the interface (because of entropic penalty and shear effect) and forms micelles which ultimately reorganize into mesophases. Whatever the intimate mechanism that leads to the continuous formation of graft copolymer, it should remain operative when PMMA−NCO is substituted for PMMA-anh of the same molecular weight. However, the interfacial reaction is apparently much slower in the case of PMMA−NCO, and only part of the process might occur within 10 min of mixing. To go a step further in the discussion, we have roughly estimated the concentration of the copolymer chains formed and supposed to reside at the interface (Σ) by eq 2 proposed by Macosko et al.[23]

$$\Sigma = (\text{chain/vol})/(\text{interface area/vol}) = (N_a \rho \phi)/(M S_{sp}) \quad (2)$$

where ρ, ϕ, and M are the density, volume fraction, and molecular weight of the copolymer, respectively, and N_a is Avogadro's number. S_{sp} is the interfacial area per unit blend volume which can be calculated from the number-average diameter (D_n) of the dispersed phases by eq 3.

$$S_{sp} = (6\phi_d)/D_n \quad (3)$$

The maximum surface concentration of the copolymer, Σ_0, can be estimated on the assumption of a dense monolayer of a symmetric diblock copolymer at a planar interface ($D_n \gg \langle r_0^2 \rangle$). The thickness of this monolayer is half the lamellae spacing (Λ/2) in the ordered bulk copolymer[26] (eq 4).

$$\Sigma_0 = \text{thickness of the copolymer monolayer/volume occupied by one chain} = (\Lambda/2)/(M/\rho N_a) \quad (4)$$

with the scaling law ($\Lambda \sim M_n^{2/3}$) valid to the strong segregation limit[26] and Λ = 39.8 nm for a dPS-PMMA

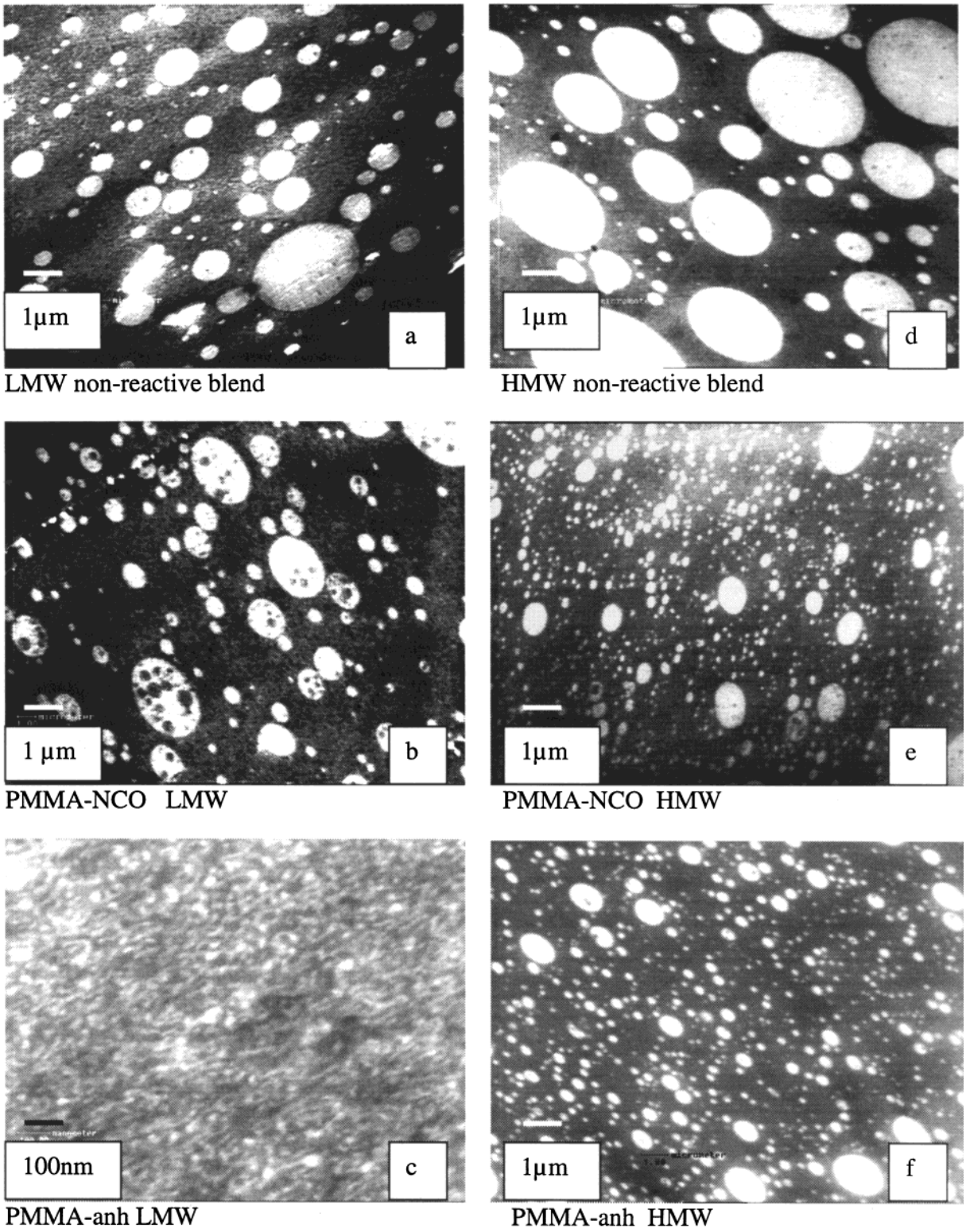

Figure 3. TEM micrographs of the morphology observed after 10 min of mixing of amine-containing PS (75 wt %) and end-reactive PMMA (25 wt %) at 170 °C: (a) blend of nonreactive low molecular weight PS and PMMA; (b) blend of low molecular weight PS-*co*-$PSNH_2$ and PMMA−NCO; (c) blend of low molecular weight PS-*co*-$PSNH_2$ and PMMA-anh; (d) blend of nonreactive high molecular weight PS and PMMA; (e) blend of high molecular weight PS-*co*-$PSNH_2$ and PMMA−NCO; (f) blend of high molecular weight PS-*co*-$PSNH_2$ and PMMA-anh. These blends were stained by RuO_4 vapors for 30 min; all the samples were cut at the same radial position from the center of the disk (20 mm).

symmetric block copolymer of $M_n = 100\ 900$ g/mol,[27] Σ_0 has been estimated for the in situ formed PS−PMMA Y-shaped graft copolymer. The estimated values (Table 3) are however upper limits, because the graft copolymer has to accommodate more severe spatial constraints and to occupy a larger interfacial area than the linear diblock of same molecular weight and composition. The extent to which the surface of the PMMA domains is covered by the in situ formed copolymer is expressed by Σ/Σ_0, a value of one being the saturation coverage (Table 3). The Σ/Σ_0 ratio is higher than 3 for the PMMA−NCO/PS-*co*-$PSNH_2$ reactive pair, which indi-

Table 3. Characterization for the Reactive Blends Formed after 10 min at 170 °C, at a Constant Radial Position[a]

original blends[b]	particle size				reaction progress[c]	interface coverage			final blend composition		
	D_v (μm)	D_n (μm)	D_v/D_n	D_v (r)/D_v(nr)	conv of NCO or anh (%)	Σ^e	$\Sigma_0{}^e$	Σ/Σ_0	copolymer (wt %)	free PMMA	free PS
HMW NCO	0.45	0.23	1.9	0.19	11	0.072	0.128	0.56	5.5[d]	22.25	72.25
HMW anh	0.40	0.20	19	0.17	20	0.1	0.128	0.78	10[d]	20	70
LMW NCO	0.90	0.38	2.38	0.54	16.5	0.62	0.203	3.1	8.2	20.9	70.9
LMW anh	–	0.025	–	0.01	92	–	0.203	–	46	2	52

[a] 20 mm from the center of the disk. [b] HMW and LMW stand for high and low molecular weight, respectively, while NCO and anh refer to reactive end group of PMMA. [c] Based on NCO or anh used in reaction with respect to the NH_2 coreactive groups. [d] Assuming that a single graft copolymer is formed. [e] In copolymer chains/nm^2.

cates a large oversaturation of the interface, consistent with a short residence time of the copolymer at the interface and accumulation in the PMMA phases. In parallel, the interfacial area has increased only two times, which suggests that the copolymer does not contribute to increase the interfacial surface area. Rather the slow formation of the copolymer and its escape from the interface are responsible for a poor phase stabilization. The phase coalescence dominates the phase breakup, which is favorable to formation of occlusions in the dispersed phases.

Blends of Reactive Precursors of Higher Molecular Weight (35 000). The molecular weight of the end-reactive PMMA and PS-*co*-$PSNH_2$ has been increased from 10 000 to 35 000. In parallel, the average number of amine per PS chain has changed from 1.2 to 4.2. Because the weight composition of the blends has been kept constant, the excess of amine with respect to isocyanate or anhydride has also increased from 4−4.5 to 15−16. If the interfacial reaction is completely random, a graft copolymer with a Y-shape should be formed preferentially. It might however happen that when one amine of a PS-*co*-$PSNH_2$ chain has reacted at the interface, a second function of the same chain is in a favorable position to react with another end-reactive PMMA chain, particularly in the case of fast reaction. If the copolymer contains more than one PMMA graft (thus more than 50 wt % PMMA), its tendency to migrate from the interface to the PMMA phase should be strongly increased.

The additional series of TEM observations (Figure 3d−f) compared to the previous one (Figure 3a−c) emphasizes the crucial role of the molecular weight of the reactive precursors. The most striking observation is that the phase morphology after 10 min of mixing does not depend anymore on the intrinsic reactivity of the functional groups (NCO/NH_2 vs anh/NH_2). Whatever the reactive group (NCO or anh) attached to the high molecular weight PMMA, the phase morphology is quite comparable (Figure 3e,f) as confirmed by the same $D_{v(r)}/D_{v(nr)}$ ratio (Table 3). Compared to the blends of the lower molecular weight chains, the phase dispersion is finer in the case of the NCO/NH_2 pair [$D_{v(r)}/D_{v(nr)} = 0.19$ instead of 0.54], and occlusions in PMMA are an exception and no longer the rule (Figure 3c). Very surprisingly, the phase dispersion is much broader for the anh/NH_2 pair ($D_{v(r)}/D_{v(nr)} = 0.17$ instead of 0.01) to the point where nanophases are not observed anymore. Consistent with the TEM observations, the progress of the interfacial reaction for 10 min of mixing is limited to 11% for NCO (vs 16.5% for the low molecular weight system) and 20% for anh (vs 92% previously). There is thus a qualitative agreement between a coarse phase dispersion, and a limited amount of copolymer formed (5.5 and 10 wt % for the NCO and anh groups, respectively; see Table 3).

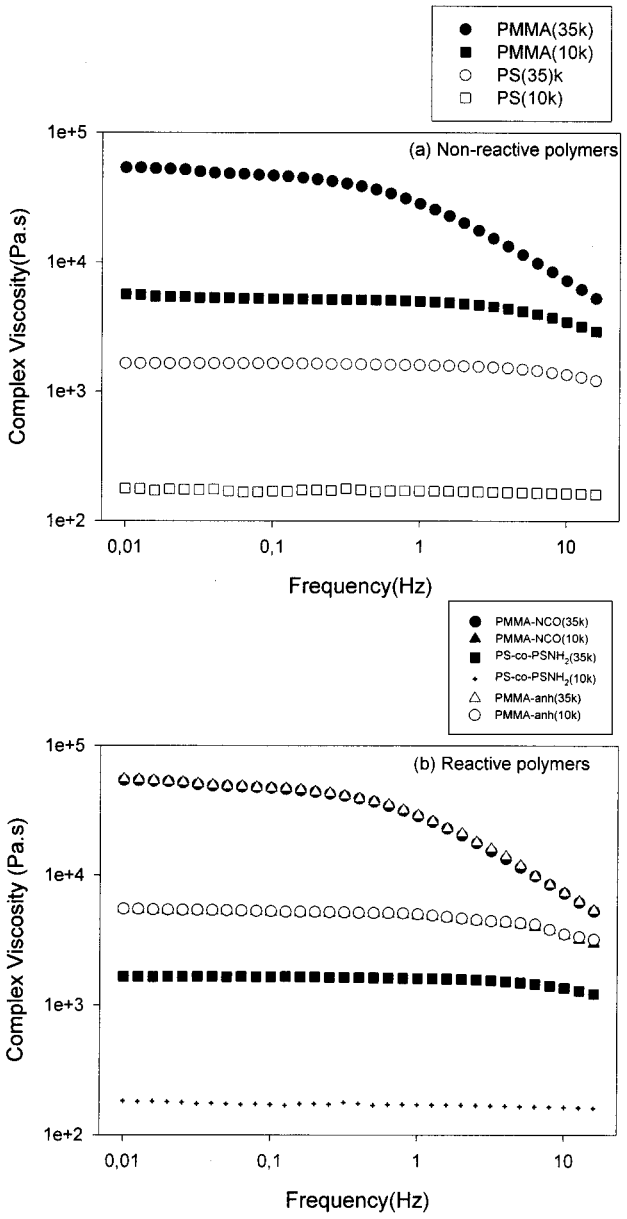

Figure 4. Rheological curves at 170 °C for nonreactive (a) and reactive (b) polymers.

The first question is to know to which extent the change in molecular weight has changed the melt viscosity of the reactive constituents and ultimately the mixing process. Figure 4 compares the complex dynamic viscosity, η^*, of the reactive and the nonreactive polymers at 170 °C. η^* is much higher for PMMA than for PS of the same molecular weight. Moreover, this property is increased by 1 order of magnitude for both PS and PMMA (e.g., at 0.1 Hz), when the molecular weight is increased from 10 000 to 35 000. The reactive groups

have no significant effect on these data. So, the relative melt viscosity at low frequency of the PS and PMMA chains is independent of their molecular weight (10 000 vs 35 000) and reactivity (reactive vs nonreactive). It is no longer the case when the phase dispersion after 10 min of mixing is concerned. Indeed, the PMMA particles are 1.4 times larger when the nonreactive chains are of higher molecular weight. The same situation prevails for the anh/NH_2 reactive system, although the amplitude of the effect is ca. 1 order of magnitude larger (comparison of D_n in Table 3). In contrast, the opposite effect is observed for the NCO/NH_2 pair, the larger PMMA particles being formed by the lower molecular weight chains. Obviously, there is no parallelism between the phase morphology of the reactive blends and the melt viscosity of the constitutive components.

In this series of blends of higher molecular weight chains, the interfacial reaction is no longer dominated by the intrinsic reactivity of the functional groups. Although the interface coverage (Σ/Σ_0) is a qualitative piece of information (more likely underestimated), it appears from Table 3 that the interface is not saturated by the graft copolymer. Furthermore, PS occlusion in PMMA is an epiphenomenon, although the content of graft copolymer is low. These indirect observations suggest that the graft copolymer does not escape from the interface significantly and that it protects the interface more effectively against coalescence. The higher melt viscosity of the dispersed PMMA phases might also restrict the particle coalescence and thus the occlusion of PS. The residence of the graft copolymer at the interface might result from the entanglements of the constitutive chain segments and the parent homopolymers of 35 000 molecular weight together with moderate shear forces. The average molecular weight between chain entanglements is indeed 10 000 for PMMA and 13 000 for PS.[28]

The increase in the molecular weight of the graft copolymer (70 000 in the case of the Y-shaped copolymer) makes it more efficient in stabilizing the interface. The problem is however that the stabilized interfacial area is not very large and that the interface is rapidly out of the unreacted chains reach. The major conclusion is that the interfacial reaction is blocked because of the very slow diffusion of the graft copolymer away from the interface. This process is thus the rate-determining step for the copolymer formation, consistent with the minor role played by the intrinsic reactivity of the chains.

Conclusion

In this work, two pairs of reactive groups (aromatic anhydride/aliphatic amine and aliphatic isocyanate/aliphatic amine) have been compared for the coupling of end-reactive (NCO or anh) PMMA and amino-containing PS, in blends containing 25 wt % PMMA and 75 wt % PS. Moreover, the molecular weight of the reactive precursors has been varied (M_n = 10 000 and 35 000). The amine content of PS and the molar excess of amine with respect to NCO (or anhydride) are such that a Y-shaped graft copolymer of a 50/50 wt composition is thought to be formed. The most striking observation is a nanophase separation and a quasi-complete reaction after 10 min of mixing at 170 °C in the specific case of the anh/NH_2 reaction at the interface formed by the lower molecular weight chains (M_n = 10 000). In all the other cases, formation of microphases is reported together with a limited progress of the interfacial reaction. When the reactive chains are of low molecular weight and cannot contribute to stable chain entanglements, the copolymer escapes from the interface which allows it to be formed as rapidly as the functional groups are mutually reactive. The chemical reaction at the interface is then the rate-determining step (isocyanate vs anhydride). If this reaction is intrinsically slow, the phase morphology is not stabilized. Indeed, the interfacial reaction cannot compensate the migration of the copolymer away from the interface, such that the development of the phase morphology is dominated by phase coalescence.

An increase in the chain length of the precursors refrains the copolymer of higher molecular weight from leaving the interface because of chain entanglements. Although the interface is better stabilized, the non yet reacted chains cannot meet further which blocks the progress of the interfacial reaction even though the functional groups are highly reactive.

Clearly the fate of the copolymer formed at the interface is kinetically controlled. Actually, the relative kinetics of two phenomena has a decisive effect on the development of the phase morphology, i.e., the interfacial reaction rate and the rate at which the interface is renewed. This kinetic balance plays a key role in the production of block or graft copolymer by reactive blending.

Acknowledgment. The authors are grateful to the "Services Fédéraux des Affaires Scientifiques Techniques et Culturelles" for general support to CERM and for a fellowship to Z.Y. in the frame of the "PAI-4/11: Supramolecular Chemistry and Supramolecular Catalysis". They thank Ms. Martine Dejeneffe for the ultramicrotomy of the samples to be observed by TEM. C.K. is "Aspirant" by the "Fonds National de la Recherche Scientifique" (F.N.R.S.).

References and Notes

(1) Koning, C.; Van Duin, M.; Pagnoulle, C.; Jérôme, R. *Prog. Polym. Sci.* **1998**, *23*, 707.
(2) Leibler, L. *Macromolecules* **1982**, *15*, 1283.
(3) Noolandi, J.; Hong, K. M. *Macromolecules* **1982**, *15*, 482.
(4) Sundararaj, U.; Macosko, C. W. *Macromolecules* **1995**, *28*, 2647.
(5) Beck-Tan, N. C.; Tai, S. K.; Briber, R. M. *Polymer* **1996**, *37*, 3509.
(6) Milner, S. T.; Xi, H. *J. Rheol.* **1996**, *40*, 663.
(7) Pagnoulle, C.; Koning, C.; Leemans, L.; Jérôme, R. *Macromolecules* **2000**, *33*, 6275.
(8) Majumbar, B.; Keskula, H.; Paul, D. R.; Harvey, N. G. *Polymer* **1994**, *35*, 4263.
(9) Nakayama, A. Master's Thesis, Department of Organic and Polymeric Materials, Tokyo Institute of Technology, 1994.
(10) Nakayama, A.; Guegan, P.; Hirao, A.; Inoue, T.; Macoscko, C. W. *ACS Polym. Prepr.* **1993**, *34* (2), 840.
(11) Ibuki, J.; Charoensirisomboon, P.; Ougizawa, T.; Inoue, T.; Koch, E.; Weber, M. *Polymer* **1999**, *40*, 647.
(12) Charoensirisomboon, P.; Chiba, T.; Solomko, S. I.; Inoue, T.; Weber, M. *Polymer* **1999**, *40*, 6803.
(13) Charoensirisomboon, P.; Inoue, T.; Weber, M. *Polymer* **2000**, *41*, 4483.
(14) Charoensirisomboon, P.; Inoue, T.; Weber, M. *Polymer* **2000**, *41*, 6907.
(15) Dedecker, K.; Groeninckx, G. *Polymer* **1998**, *39*, 4993. Dedecker, K.; Groeninckx, G. *Pure Appl. Chem.* **1998**, *70*, 1289.
(16) Luzinov, I.; Julthongpiput, D.; Malz, H.; Pionteck, J.; Tsukruk, V. V. *Macromolecules* **2000**, *33*, 1043.
(17) Timothy, E. P.; Matyjaszewski, K. *Adv. Mater.* **1998**, *12*, 10.
(18) Keller, R. N.; Wycoff, H. D. *Inorg. Synth.* **1946**, *2*, 1.
(19) Haddelton, D.; Waterson, C.; Derrick, P. J.; Jasieczek, C. B.; Hannon, M. J.; Schooter, A. J. *Chem. Commun.* **1997**, 683.

(20) Dexter, R. W.; Saxon, R.; Fiori, D. E. *J. Coat. Technol.* **1986**, *58*, 43.
(21) Hu, G. H.; Kadri, I. J. *J. Polym. Sci., Part B: Polym. Phys.* **1998**, *36*, 2153.
(22) Guégan, P.; Macosko, C. W.; Ishizone, T.; Hirao, A.; Nakahama, S. *Macromolecules* **1994**, *27*, 4993.
(23) Macosko, C. W.; Guégan, P.; Khandpur, A. K.; Nakayama, A.; Maréchal, P.; Inoue, T. *Macromolecules* **1996**, *29*, 5590.
(24) Pagnoulle, C.; Koning, C. E.; Leemans, L.; Jérôme, R. *Macromolecules* **2000**, *33*, 6275.
(25) Orr, C. A.; Adedeji, A.; Hirao, A.; Bates, F. S.; Macosko, C. W. *Macromolecules* **1997**, *30*, 1243.
(26) Bates, F. S.; Fredrickson, G. H. *Annu. Rev. Phys. Chem.* **1990**, *41*, 525.
(27) Russel, T. P.; Menelle, A.; Hamilton, W. A.; Smith, G. S.; Satija, S. K.; Majkrzak, C. F. *Macromolecules* **1991**, *24*, 5721.
(28) Fetters, L. J.; Lohse, D. J.; Richter, D.; Witten, T. A.; Zirkel, A. *Macromolecules* **1994**, *27*, 4639.

MA001798+